Case Studies in Thermal Engineering 9 (2017) 28–39

Contents lists available at ScienceDirect

Case Studies in Thermal Engineering

journal homepage: www.elsevier.com/locate/csite

Energy and parametric analysis of solar absorption cooling systems in various Moroccan climates

Y. Agrouaz[a,b,*], T. Bouhal[a,b], A. Allouhi[a], T. Kousksou[b], A. Jamil[a], Y. Zeraouli[b]

[a] École Supérieure de Technologie de Fès, Université Sidi Mohamed Ben Abdellah, Route d'Imouzzer, BP 242, Fez, Morocco
[b] Laboratoire des Sciences de l'Ingénieur Appliquées à la Mécanique et au Génie Electrique (SIAME) Université de Pau et des Pays de l'Adour – IFR – A. Jules Ferry, 64000 Pau, France

ARTICLE INFO

Keywords:
Solar cooling system
Absorption
Performance
Morocco

ABSTRACT

The aim of this work is to investigate the energetic performance of a solar cooling system using absorption technology under Moroccan climate. The solar fraction and the coefficient of performance of the solar cooling system were evaluated for various climatic conditions. It is found that the system operating in Errachidia shows the best average annual solar fraction (of 30%) and COP (of 0.33) owing to the high solar capabilities of this region. Solar fraction values in other regions varied between 19% and 23%. Moreover, the coefficient of performance values shows in the same regions a significant variation from 0.12 to 0.33 all over the year. A detailed parametric study was as well carried out to evidence the effect of the operating and design parameters on the solar air conditioner performance.

1. Introduction

The energy use in buildings is exponentially growing [1]. Vapor compression air-conditioning systems used in building cause a significant consumption of electrical energy in many parts of the world. Currently, the cooling demand is expected to increase because of increased comfort standards and worldwide warming issues. For instance, 40% of electricity production during summer is entirely used by US commercial buildings for air-conditioning purposes [2]. In Egypt, 32% of the electricity is consumed by air-conditioning in the domestic sector [3].

Vapor compression chillers use different types of refrigerants such as Chloro-Flouro-Carbon and Hydro-Chloro-Flouro-Carbo with high negative impact on the environment. Therefore, it is suitable to decrease or at least prevent the use of these refrigerants [4].

To improve the energy efficiency in buildings, solar air-conditioning seems to be an interesting alternative to reduce electricity consumption, especially during summer, when cooling loads coincide generally with availability of solar irradiation.

The technologies of solar cooling using sorption principle such as absorption or adsorption are commercialized by many companies in different sizes because of their relatively high performances compared to other systems [5]. Pons et al. [6] reported the experimental performances over all seasons and on one single day of six chillers using five different technologies and in five different locations. They found that the performances evaluated on one single day can be over-estimated (+30%) compared to seasonal averages, the difference between the two methods can be theoretically interpreted as a non-linear effect related to the thermal inertia of the solar field.

Abbreviations: CFC, Chloro-Flouro-Carbon; HCFC, Hydro- Chloro-Flouro-Carbon; LiBr, Lithium bromide; DHW, Domestic hot water; ADEREE, Agence Nationale pour le Développement des Energies Renouvelables et de l'Efficacité Energétique; COP, Coefficient of Performance

* Corresponding author.

http://dx.doi.org/10.1016/j.csite.2016.11.002
Received 22 June 2016; Received in revised form 25 September 2016; Accepted 6 November 2016
Available online 12 November 2016

Nomenclature

A	Area [m^2]
c_p	Specific heat at constant pressure [J kg^{-1} $°C^{-1}$]
G	Solar radiation [W m^{-2}]
Q	Heat (J)
T	Temperature [°C]
m	Mass flowrate [kg/h]
F_R	Collector heat removal factor [-]
U_L	Heat loss coefficient [W/m^2 K]
g	g-value[-]

Greek letters

η	Collector efficiency [-]
τα	Transmittance–absorbance product

Subscripts

avg	Average
amb	Ambient
s	Solar
aux	Auxiliary
c	Collector
evap	Evaporator
gen	Generator

Al-Ugla et al. [7] studied a three alternative design (heat storage, cold storage, and refrigerant storage) of a 24 h operating solar absorption system in Saudi Arabia in order to determine the best suitable alternative, their analysis revealed that alternative design with refrigerant storage of a solar LiBr/H_2O absorption system is the best alternative because of its high coefficient of performance (of 0.77) with a small collector size (22 m^2) compared to other alternatives.

Calise et al. [8] presented a technical and economic feasibility of a novel solar cooling system based on a new and innovative flat-plate evacuated solar thermal collector and using a double-effect absorption chiller. The experiment results show that collector peak efficiency is over 60% and daily average efficiency is around 40% and they indicate that systems equipped with flat-plate evacuated solar collectors reach a higher solar fraction (77%) compared to 66.3% for PTC collectors. In Australia, an energetic, economic and environmental analysis of LiBr-H_2O absorption chiller is conducted by Shirazi et al. [9] simulating four configurations of solar heating and cooling systems. The results show that the second configuration which consisted of an absorption chiller with a mechanical compression chiller working as an auxiliary cooling system, reached a solar fraction of 71.8% and primary energy savings of 54.51%. Tsoutsos et al. [10] conducted a parametric study concerning the economic evaluation of two types of solar cooling systems (absorption and adsorption) in Greece. They compared economically the performance of these two technologies to the traditional air-conditioner taking into account several indicators such as the initial cost of primary energy, carbon taxes and energy inflation.

Vasta et al. [11] presented a dynamic simulation and a performance analysis of an adsorption chiller operating under three different cities in Italy. They concluded that the design parameters have a significant influence on the performance indicators. They found that the solar fraction can reach 81% and 50% for the two types of cooler (Dry and Wet) at a lower number of solar collectors. In addition, it was found that the COP of the adsorption chiller can achieve values of 57% and 35% for the same configuration of collectors.

In UAE, Al-Alili et al. [12] conducted a numerical study of an absorption solar cooling system to evaluate its performance. They studied a novel solar air cooling system which consists of hybrid air conditioner and hybrid photovoltaic/thermal solar collectors. They found that the COP of the investigated system is higher than that of an absorption solar chiller. The related average cooling COPs are found to be 0.68 and 0.29, respectively.

Morocco possesses an important potential of solar energy [13,14]. In fact, the average daily solar radiation is about 5.3 kW h/m^2 with more than 5000 h of sunshine annually. Accordingly, the development of solar-air conditioning in Morocco seems to be of a great importance and is within the new government strategies for the promotion of renewable energy projects [15].

The main objective of this work is to provide useful guidelines about the operation of solar cooling systems under Moroccan climate. In this sense, an energy analysis and performance evaluation of a solar-air conditioning system was carried out. Optimal design of the system is reported as well.

2. Design aspects

2.1. Thermal solar cooling system

The solar cooling plant under investigation can be divided into two subsystems: the solar subsystem and the cooling subsystem. The first one includes solar collectors, a heat exchanger, a thermally insulated hot storage tank, an electrical auxiliary heater, two circulating pumps and a distribution circuit. The second one integrates an absorption chiller, a cooling tower, a cold storage tank, and three pumps connected respectively to the generator, evaporator and condenser. The schematic diagram of the overall solar cooling system is shown in Fig. 1.

A flat-plate collector transfers the energy collected from the solar irradiation to a solar tank through an external exchanger. The primary and secondary pumps coupled respectively, the solar field to the heat exchanger and the storage tank to the solar collectors. The thermal energy stocked in the tank flows to the absorption chiller that produces chilled water, then the chilled water is injected into a water/air exchanger to cool the building.

It is clear from Fig. 1 that the solar installation can additionally provide space heating and domestic hot water (DHW) production. However, only the results concerning solar air-conditioning are reported in this study.

2.1.1. Solar collector field

The solar collector field used in the solar cooling plant is based on flat-plate technology. The average value of the specific collector area for an absorption chiller is 2.5 m^2/kW cold [16]. The nominal cooling capacity of the proposed absorption chiller is 10 kW, the area of the solar field required is therefore 25 m^2. The useful heat of the collectors is given by:

$$Q_{useful} = mc_p(T_0 - T_i) = AF_R[G(\tau\alpha) - U_L(T_{avg} - T_{amb})] \quad (1)$$

where F_R is the collector heat removal factor. It is the ratio of the actual collector useful heat to that of the collector at a uniform temperature which is equivalent to inlet fluid temperature. Since the heat loss coefficient is not actually constant, a linear dependency is assumed as shown in the following equation:

$$F_R U_L = a_1 + a_2(T_{avg} - T_{amb}) \quad (2)$$

Thus, the thermal collector efficiency is based on the standard second-order collector performance given by:

$$\eta = \eta_0 - a_1\frac{(\Delta T_{avg})}{G} - a_2\frac{(\Delta T_{avg})^2}{G} \quad (3)$$

The η_0 parameter indicates the optical efficiency of the collector; a_1 and a_2 present respectively thermal loss parameters. G is solar radiation, ΔT_{avg} is the difference between the mean temperature across the solar collector and the ambient temperature. The technical specifications of the solar collector are listed in Table 1.

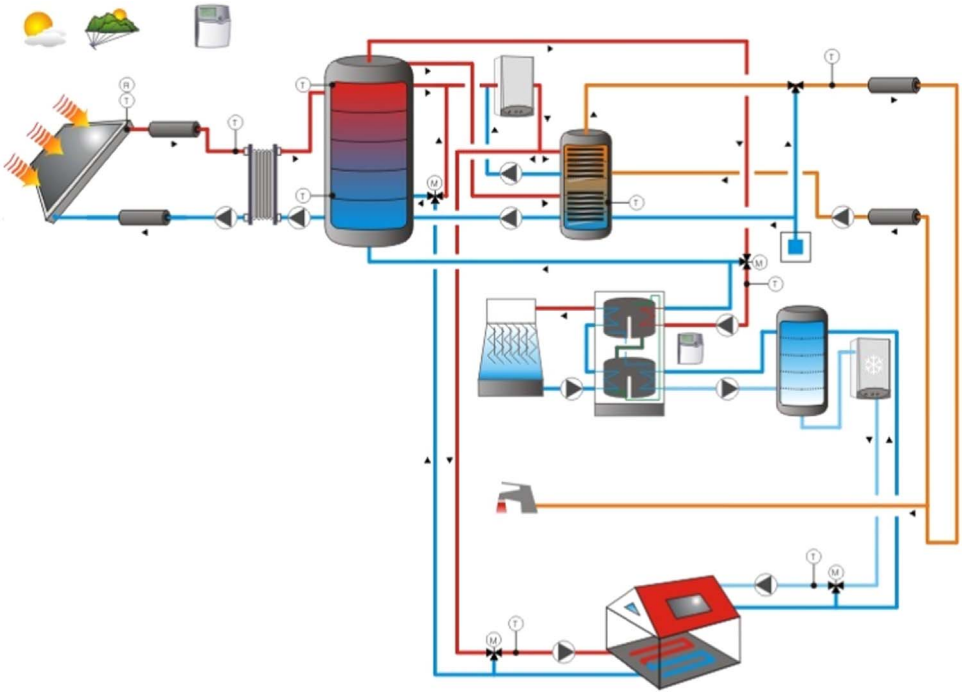

Fig. 1. Schematic of the solar cooling system.

Table 1
Characteristics of the collector.

Parameters	Value FCP	Unit
η_0	0.85	–
a_0	4.07	W/m^2 K
a_1	0.007	W/m^2 K^2

2.1.2. Solar storage tank

According to [17], the volume of the storage tank (expressed in liters) should be at least 50 times of the collector surface (in m^2) for common consumption profile. On this basis, a 1250 L storage tank is selected.

2.1.3. Cooling tower

Generally, the air flow rates ranging between 130 m^3/h and 170 m^3/h per a kW of cooling capacity are recommended for the design of cooling towers in cooling applications. Therefore, a flow rate of 1500 m^3/h is considered in this study. Moreover, since the consumption of the fan varies from 6 kW to 10 kW and from 10 kW to 20 kW per kW of cooling capacity respectively, for axial and radial fans according to [16], a 40 kW axial cooling tower is retained.

2.1.4. Thermal chiller

The absorption chiller used in this simulation has a cooling capacity of 10 kW. A backup chiller of 5 kW is also used in order to cover the cooling load of the described building when the thermal resource is not sufficient to drive the absorption chiller. The control strategy of the thermal chiller and cold distribution system are summarized in Table 2.

2.1.5. Solar loop control

The primary and the secondary pumps are not simultaneously activated. The primary loop is activated if the irradiation is over 300 W/m^2 and deactivated if it is under 250 W/m^2. The maximum temperature in primary loop and storage tank is respectively 102 °C and 90 °C. The secondary pump works when the difference between the tank bottom temperature and the temperature at the collector outlet reaches 11 °C, and it turns off when this difference is less than 5 °C.

2.2. Weather data

Morocco is segmented into six climatic zones; each zone is represented by a reference city. This segmentation was developed by ADEREE (*Agence Nationale pour le développement des énergies renouvelables et de l'efficacité énergétique*) and the National Center of Meteorology in order to establish a new thermal building regulation [18]. Table 3 summarizes the main characteristics of the climatic zones. The climatic data for Marrakech city are generated by Meteonorm database and are presented in Fig. 2.

2.3. Description of the building

The selected building is a one floor building with a reference surface of 200 m^2 including walls and windows. The building is oriented east–west axis. The characteristics of this building are given in Tables 4–5. The properties of the construction are selected based on the available construction types predefined in TRANSOL (see Table 6). The computed cooling loads taking into account several factors such as external and internal gains, occupancy and climatic data are plotted in Fig. 3. Table 7 gives different details of energy gains for the building under investigation [19–21].

Table 2
Controls of the thermal chiller and cold distribution system.

Cold distribution system	Thermal chiller control strategy
Emission system: fans	Thermal chiller set point: 10 °C.
Control temperature: 26 °C	Generator set point temperature: 75 °C.
Return temperature: 17 °C	Generator dead band: 5 °C.
Maximum flow rate: 36000 kg/h	Thermal chiller minimum cooling temperature: 28 °C

Table 3
Coordinates of the six zones.

Climatic sites	Reference city	Coordinates
Zone1	Agadir	30° 25′ North 9° 36′ W
Zone2	Tangier	35° 46′ N 5° 48′ W
Zone3	Fez	34° 03′ N 4° 58′ W
Zone4	Ifrane	33° 32′ N 5° 06′ W
Zone5	Marrakech	31° 37′ N 8° 00′ W
Zone6	Errachidia	31° 55′ N 4° 25′ W

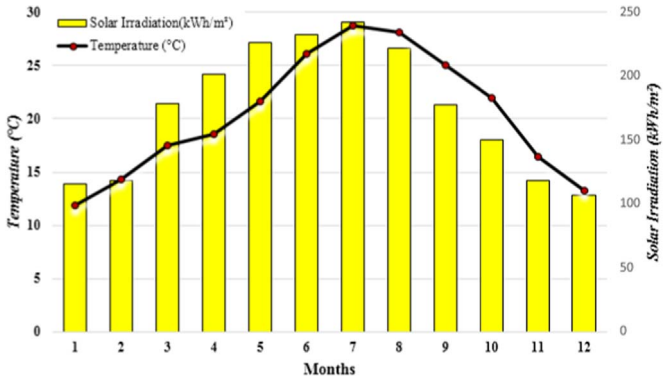

Fig. 2. Solar irradiation and ambient temperature in the Marrakech zone.

Table 4
Characteristics of the building walls.

Wall orientation	Glazed area	Unit
North	37.39	%
West	–	–
East	10	%
South	37.39	%

Table 5
Properties of the building.

Building properties	Values	Unit
Number of floors	1	–
Height of floor	2	m
Longest wall	20	m
Rotation of the building	0	°

Table 6
Thermal properties of walls and windows.

Type of wall	Value	Unit
U	0.24	W/m^2 k
Type of windows		
U	2.26	W/m^2 k
G	0.678	–

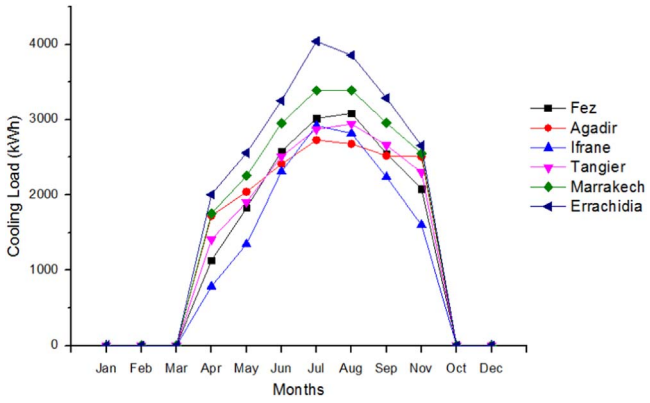

Fig. 3. Cooling loads for the six cities.

Table 7
Internal loads.

Internal loads	Value	Unit
Infiltration	0.2	1 h^{-1}
Mechanical ventilation	0.34	1 h^{-1}
Relative humidity	50	%
Specific gain (equipment and people)	15	W/m^2
Specific lightning	15	W/m^2
Occupation rate	0.05	Occupants/m^2
Sun protection	Deactivated	–

3. Performance analysis

3.1. Solar fraction

The performance of solar cooling systems can be assessed using the solar fraction. This factor shows the contribution of solar energy in the production of chilled water [22]. The solar fraction is calculated by the following equation:

$$SF = \frac{Q_s}{Q_s + Q_{aux}} \tag{4}$$

where Q_s is solar gain and Q_{aux} is auxiliary heating requirement.
Q_s can be evaluated by

$$Q_s = Q_c - \sum Q_{loss} \tag{5}$$

where Q_c is useful energy of the collectors and Q_{loss} characterizes energy losses in the solar and cooling subsystems.

3.2. Coefficient of performance COP

The coefficient of performance (COP) represents the ratio of the energy absorbed in the evaporator (causing cooling effect) denoted Q_{evap} to the energy supplied by the generator (Q_{gen}). In other words, it is the ratio of production of chilled water to the consumption of hot water [23]. The following relationship permits the calculation of the COP:

$$COP = \frac{Q_{evap}}{Q_{gen} + Q_{aux}} \tag{6}$$

Q_{aux} is the energy consumed by the auxiliary equipment.

4. Simulation results and discussion

In this section, the thermal performance of the solar cooling system is carried out through the evaluation of solar fraction and COP described in Section 3.

Figs. 4 and 5 give respectively, the solar fraction and COP over the year, for six simulated cases corresponding to various climatic zones in Morocco. The comparison based on evaluation of the COP indicates that the system operating in Agadir has the highest average COP (a value of 0.26). In the opposite, the system under Ifrane conditions, presents the lowest average COP (0.19). In the

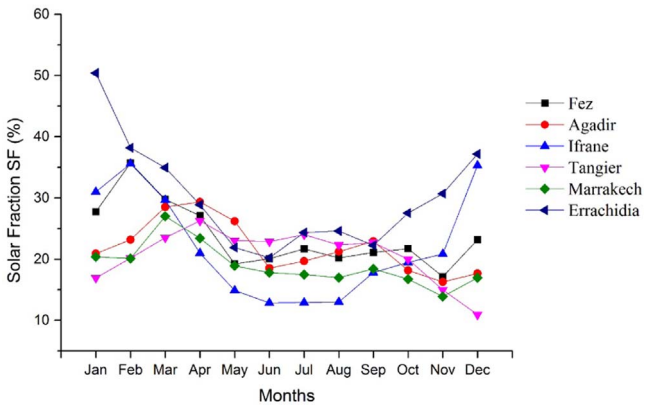

Fig. 4. Solar fraction in the six Moroccan cities.

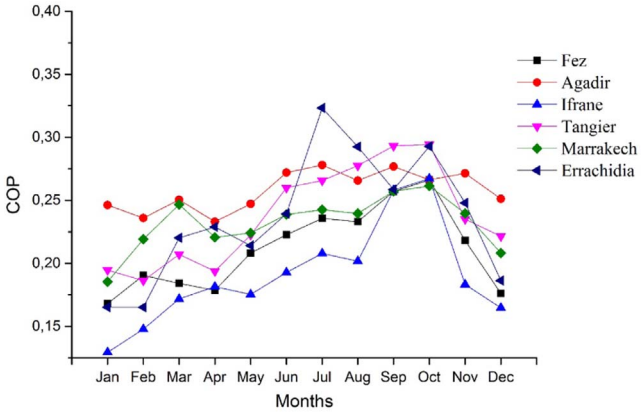

Fig. 5. COP in the six Moroccan zones.

other cities (Fez, Marrakech, Errachidia and Tangier), the average COP ranges between 0.19 and 0.26. It is also found that the system under operating in Errachidia gives the best average annual solar fraction (of 30%) due to the high solar potential of this region. Solar fraction values in other cities ranged between 19% and 23%. This result reflects the influence of solar irradiation on energetic performances of solar cooling systems.

It is clearly seen that there is a significant influence of climatic data of each zone on the solar fraction, especially, the solar irradiation which has a direct impact on the thermal energy produced by the collector field. This can be also observed, referring to Eq. (4).

Based on Eq. (6), it can be concluded that the difference in coefficient of performance (Fig. 5) between the six zones is reported directly to thermal energy at the inlet and outlet of both generator and evaporator of the absorption machine. The performance of the absorption machine depends strongly on energy flows within these two components. Generally, the generator is affected by the solar radiation of each zone while the evaporator is influenced by the cooling loads of the concerned building which depend on the outdoor temperature of each zone.

4.1. Temperature profiles

The simulation was carried out for FPC technology. The thermal behavior of collector, hot storage tank, collector, generator and evaporator of the absorption machine are presented. For a representative and detailed analysis, two consecutive days referring to the coldest and hottest days of the year in Marrakech were considered.

Fig. 6 shows simultaneously the hourly evolution of ambient temperature, outlet temperature from the solar collector field, top temperature of the solar tank, temperature at the generator inlet, temperature at the evaporator outlet and the indoor building temperature. The simulation results refer to the two coldest days of the year (February 15–16). It is clearly seen that the ambient temperature, during this period is at its lowest annual values. During the night, the ambient temperature is around 10 °C, and during the morning, it augments gradually to reach its maximum daily value of 20 °C. It can be also seen that the outlet temperature of collector increases when solar irradiation is important, this affects as well the temperature of the solar tank.

Fig. 7 presents the same temperature profiles of the parameters presented in Fig. 6 but this time during the hottest period of the year referring to July 21–22. The difference that can be noticed is that the outlet temperature from the collector, solar tank temperature and inlet generator temperature are higher compared to the previous case because of a significant solar irradiation available in summer. Moreover, Figs. 6 and 7 outline also the inlet and outlet points of the absorption chiller. They clearly explicit the hot water driving temperature, which was set at 75 °C and chilled water temperature of 10 °C that was achieved during the steady state period. It is clearly seen that the inlet generator temperature has approximately the same behavior of the top storage tank temperature since the hot water tank feeds directly the machine generator. Also, it is seen that evaporator outlet temperature remains constant during the considered period, which means that the cooling system provides a continuous cooled air to the building all over the day. These results are consistent with results simulated and reported in previous works [9,24].

4.2. Parametric analysis

4.2.1. Effect of collector tilt angle

The tilt angle of the thermal collector field has a major effect on the overall performances of the solar cooling system. Fig. 8 shows the effect of collector slope on incident solar irradiation in Marrakech. The simulation based on a variation of the slope angle from 10 to 60 degrees by a step of 10 degrees, was conducted in order to determine the optimum angle which gives the highest annual incident solar irradiation. The variation of this parameter shows that the first three months give a lower solar incident irradiation for small angle values (10° and 20°) and also the same behavior can be observed for the last three months of the year.

The higher inclination angles (30°, 40°, 50°, 60°) give a higher solar incident irradiation during winter contrarily to summer

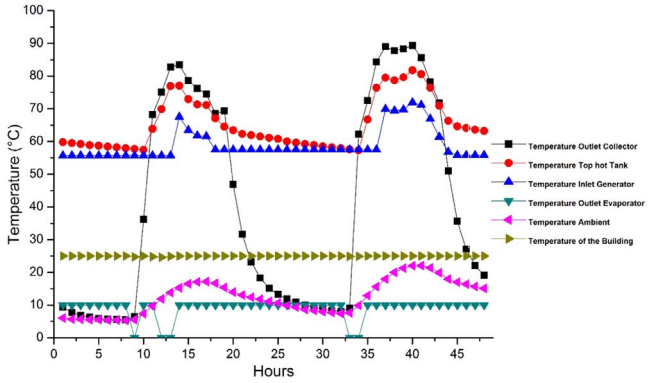

Fig. 6. Temperatures evolution during the coldest days (Feb 15–16) in Marrakech.

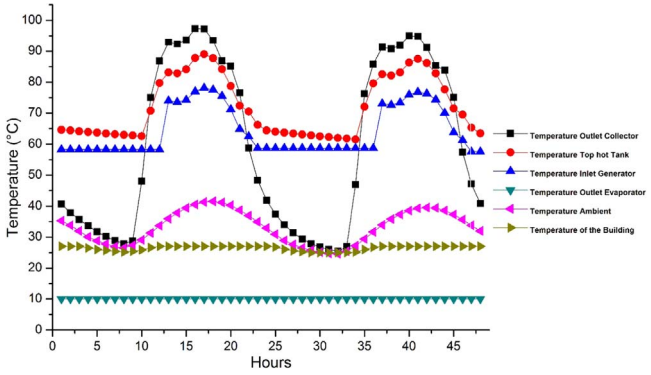

Fig. 7. Temperatures evolution during the hottest days (Jul 21–22) in Marrakech.

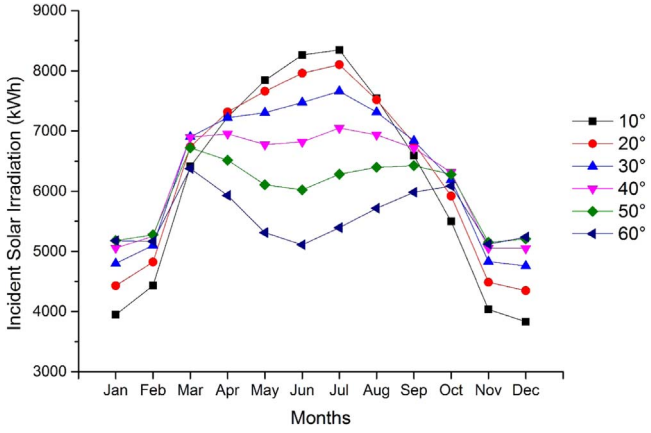

Fig. 8. Effect of the inclination angle of the solar collector (Marrakech).

where it decreases. The annual average incident solar irradiation over all the year for different inclination angles is displayed in Table 8. It is shown that the optimum angle values giving higher solar irradiations are between 30° and 40°.

As an example, a flat-plate collector operating in Marrakech and tilted at an angle of 10 degrees presents an incident solar irradiation that reaches 4000 kWh and 9000 kWh respectively in January and July months. At an angle of 40, it reaches 5000 kWh and 7900 kWh for the same months.

The difference is due to the perpendicularity of solar radiation that gives optimum results in summer with low values of tilt angles, but during winter, the optimum results are obtained for high values of collector tilt angles because of the low sun altitude during these months as reported by [25,26].

Therefore, working with an optimal value for inclination angles can easily enlarge the amount the incident solar energy and therefore increase the thermal and economic efficiency of the solar cooling system.

Table 8
Annual average solar incident irradiation for different inclination angles.

(kWh)	10°	20°	30°	40°	50°	60°
Fez	6186.837	6395.813	6449.407	6347.161	6092.519	5694.839
Agadir	6302.387	6491.206	6522.788	6397.402	6118.618	5697.191
Tangier	6122.965	6366.634	6455.122	6386.856	6164.456	5795.699
Ifrane	6690.232	6943.741	7026.599	6937.302	6679.299	6262.053
Marrakech	6165.313	6342.054	6367.412	6239.077	5964.269	5550.838
Errachidia	7196.061	7473.760	7561.813	7460.865	7171.949	6708.256

4.2.2. Effect of collector surface

Sizing a solar cooling installation requires the determination of the optimum configuration of the solar field. The collector surface has a significant influence on the performance and economic viability of a solar cooling system. Several simulations were launched to determine the effects of this parameter on the overall performance of the studied solar cooling plant.

Fig. 9 depicts the solar fraction variation of the solar cooling system for different surfaces of collector field. The dynamic simulation consists of changing the collector surface from 20 m^2 to 80 m^2 by a step of 10 m^2. Climatic data of Marrakech are employed as inputs for the simulations.

Increasing the solar field surface shows an enhancement of the solar fraction because of the proportion between the monthly solar fraction and the energy collected from the solar field. Based on the results depicted in Fig. 9, it is observed that the solar fraction remains practically constant at high surfaces of the solar collector field (> 60 m^2). For the summer period, the studied system shows a solar fraction of nearly 10% for 20 m^2 and 25% for 60 m^2. This stability in the solar fraction that was also obtained by other published works [27,28] indicates that the system reaches its optimum and any further augmentation of the surface field leads to an over production of thermal energy which can causes technological issues and increase considerably the initial investment.

4.2.3. Effect of storage tank size

The non-continuous aspect of solar energy can cause an interruption in the cold supply during nights. Thus, a thermal storage tank is necessary. This section investigated the effect of the storage tank size on the annual solar fraction for the studied zone.

Fig. 10 shows the variation of the solar fraction throughout the year for different tank sizes. The tank size was varied from 500 L to 3000 L by a step of 500 L. The simulation results show a small variation of solar fraction. In fact, for January a high storage tank size (1500–3000 L) and lower storage tank size (100–1000 L) gives a solar fraction of 18% and 21% respectively. This difference (3%) indicates that the variation of storage tank size has not a significant effect on the solar fraction. However, a high storage size shows a better value of the solar fraction during summer because of a high production of hot water contrarily, at winter, the low solar irradiation decreases directly the production of hot water, therefore a lower storage size gives a better performance. Moreover, all the storage tank has the same technical characteristics. Therefore, a high storage tank size increases the thermal energy losses that influences the solar fraction of the system, especially during winter months when the surrounding temperature is significantly low.

4.2.4. Effect of evaporator mass flow rate

The evaporator is the component where the cold water production takes place. It is connected to a water/air exchanger to cool the desired space of the building. A set of simulations is carried out to pertain the effect of evaporator or chilled water flow rate on the cooling production of the thermal chiller. The evaporator flow rate was varied from 1600 kg/h to 2100 kg/h. The obtained results for Marrakech climate are shown in Fig. 11.

An increase in the evaporator flow rate augments the production of chilled water. In fact, for January (beginning of the winter season) the solar cooling production presents a lower monthly value of 130 kWh for all investigated flow rates because of lower solar

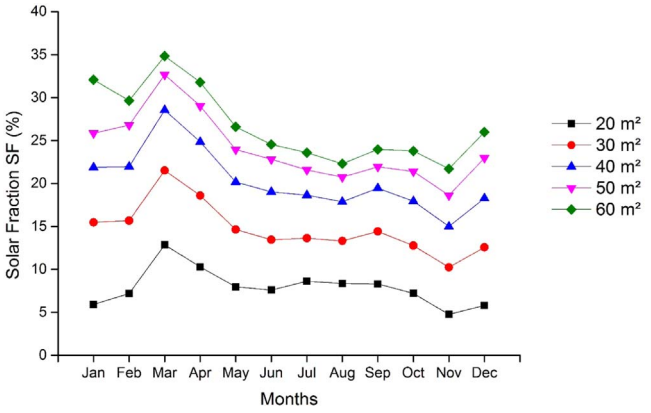

Fig. 9. Effect of the collector surface on the solar fraction (Marrakech).

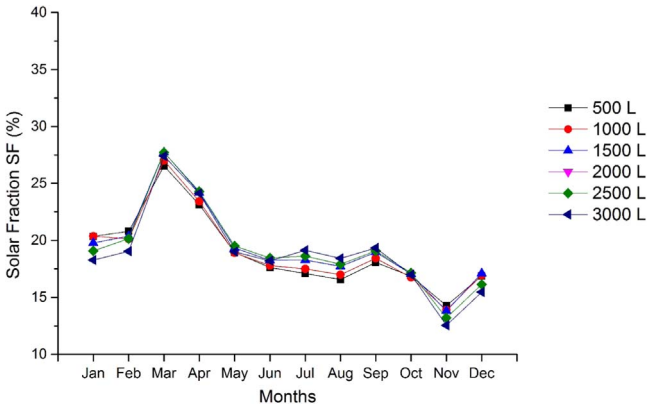

Fig. 10. Effect of the storage tank size on the solar fraction (Marrakech).

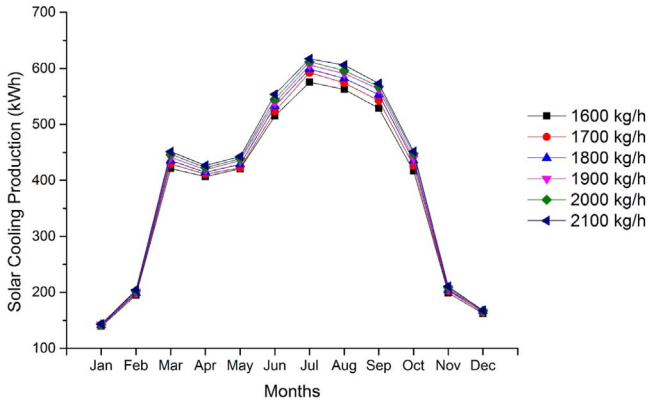

Fig. 11. Effect of the evaporator flow rate on the solar cooling production (Marrakech).

irradiation. The effect of the evaporator flow rate is clearly seen at the beginning of summer, where the solar cooling production shows an important improvement (400 kWh and 450 kWh for 1600 kg/h and 2100 kg/h respectively, for the month of April). A peak value of 600 kWh for a flow rate of 2100 kg/h is observed in July when the solar potential is higher.

From the above results, it can be recommended to control the flow rate value in the evaporator in such a way to provide higher values in the summer hottest month when the cooling demand is significantly high. This will adjust the cooling capacity of the absorption machine and lead to a higher performance.

4.2.5. Effect of generator mass flow rate

The last set of simulations evidences the effect of the generator flow rate. From Fig. 12, it can be seen that the cooling production of the solar absorption chiller increases while increasing the generator flow rate. In fact, during winter, when the solar irradiation is

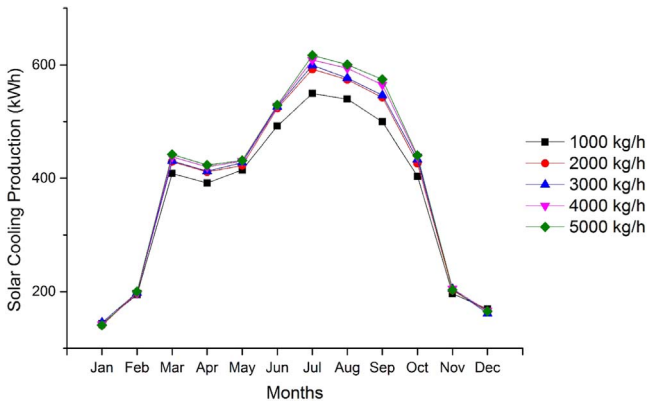

Fig. 12. Effect of the generator flow rate on the solar cooling production (Marrakech).

low, cooling production shows a small value (100 kWh and 130 kWh for January and December, respectively) contrarily to hot months, in which the effect of generator flow rate is more pronounced. For example, a flow rate of 1000 kg/h and 5000 kg/h give a solar cooling production of 500 kWh and 600 kWh respectively.

In fact, the production of chilled water can be increased by increasing the flow rate of the generator. This is an obvious result of the increase of the thermal energy received by the absorption chiller since hot water at higher flow rate is injected into the chiller machine through the generator, then the absorption cycle starts and cooled water is produced and used via the evaporator outlet.

5. Conclusion

The current study presented a detailed performance analysis of a solar air-conditioning system operating under Moroccan climate. Different parameters affecting the solar fraction and the solar cooling production of the investigated system were discussed.

According to the simulation results, it was shown that the climatic conditions influence significantly the performance of the solar cooling system. During peak-load months, Errachidia presented the highest performance. The corresponding COP reached a value of 0.3 while the solar fraction was 45%.

The results of the parametric analysis evidenced the best design configuration of solar cooling plant. It was found that inclination angle has a significant influence on the solar incident irradiation. An optimum value (between 30% and 35% for the case of Marrakech) of collectors slope leads to higher performances. The analysis of the surface collectors showed that generally, increasing the collector surface field leads to better values of the fraction. It is also found that the solar fraction was unchanged for an area greater than 50 m^2. It is therefore concluded that the selection of appropriate surface of collector needs to be carried out along with an economical and technical viability (mainly cost-analysis and land availability) to ensure the best system profitability.

On the other hand, the variation of the storage tank size does not present a significant influence on solar fraction (18% and 21% for 500 L and 3000 L, respectively).

Both increasing evaporator and generator flow rates enhance the solar cooling production during the hot summer months when the available solar radiation and the cooling loads are significantly important.

Finally, this study presents guidelines for designers, in order to take into consideration the effect of all the investigated design and operating parameters while establishing solar cooling system operating under Moroccan climate.

Acknowledgments

The authors acknowledge the support provided by the "Institut de Recherche en Energie Solaire et Energies Nouvelles (IRESEN)" under the project of Solar Cooling Process in Morocco (SCPM).

References

[1] A. Allouhi, Y. El Fouih, T. Kousksou, A. Jamil, Y. Zeraouli, Y. Mourad, Energy consumption and efficiency in buildings: current status and future trends, Journal of Cleaner Production 109 (2015) 118–130.
[2] A. Syed, G.G. Maidment, J.F. Missenden, R.M. Tozer, An efficiency comparison of solar cooling schemes/Discussion, ASHRAE Transactions 108 (2002) 877.
[3] A. Elsafty, A.J. Al-Daini, Economical comparison between a solar-powered vapour absorption air-conditioning system and a vapour compression system in the Middle East, Renewable Energy 25 (4) (2002) 569–583.
[4] A. Allouhi, T. Kousksou, A. Jamil, T. El Rhafiki, Y. Mourad, Y. Zeraouli, Economic and environmental assessment of solar air-conditioning systems in Morocco, Renewable and Sustainable Energy Reviews 50 (2015) 770–781.
[5] A. Allouhi, T. Kousksou, A. Jamil, Y. Agrouaz, T. Bouhal, R. Saidur, A. Benbassou, Performance evaluation of solar adsorption cooling systems for vaccine preservation in Sub-Saharan Africa, Applied Energy 170 (2016) 232–241.
[6] M. Pons, G. Anies, F. Boudehenn, P. Bourdoukan, J. Castaing-Lasvignottes, G. Evola, D. Stitou, Performance comparison of six solar-powered air-conditioners operated in five places, Energy 46 (1) (2012) 471–483.
[7] A.A. Al-Ugla, M.A.I. El-Shaarawi, S.A.M. Said, Alternative designs for a 24-h operating solar-powered LiBr–water absorption air-conditioning technology, International Journal of Refrigeration 53 (2015) 90–100.
[8] A. Buonomano, F. Calise, M.D. d'Accadia, G. Ferruzzi, S. Frascogna, A. Palombo, M. Scarpellino, Experimental analysis and dynamic simulation of a novel high-temperature solar cooling system, Energy Conversion and Management 109 (2016) 19–39.
[9] A. Shirazi, R.A. Taylor, S.D. White, G.L. Morrison, Transient simulation and parametric study of solar-assisted heating and cooling absorption systems: An energetic, economic and environmental (3E) assessment, Renewable Energy 86 (2016) 955–971.
[10] T. Tsoutsos, J. Anagnostou, C. Pritchard, M. Karagiorgas, D. Agoris, Solar cooling technologies in Greece. An economic viability analysis, Applied Thermal Engineering 23 (11) (2003) 1427–1439.
[11] S. Vasta, V. Palomba, A. Frazzica, F. Costa, A. Freni, Dynamic simulation and performance analysis of solar cooling systems in Italy, Energy Procedia 81 (2015) 1171–1183.
[12] A. Al-Alili, M.D. Islam, I. Kubo, Y. Hwang, R. Radermacher, Modeling of a solar powered absorption cycle for Abu Dhabi, Applied Energy 93 (2012) 160–167.
[13] A. Allouhi, A. Jamil, T. Kousksou, T. El Rhafiki, Y. Mourad, Y. Zeraouli, Solar domestic heating water systems in Morocco: an energy analysis, Energy Conversion and Management 92 (2015) 105–113.
[14] A. Allouhi, R. Saadani, T. Kousksou, R. Saidur, A. Jamil, M. Rahmoune, Grid-connected PV system installed on institutional buildings: Technology comparison, energy analysis and economic performance, Energy and Buildings 133 (2016) 188–201.
[15] Ministère de l´Energie, des Mines, de l´Eau et de l´Environnement. Stratégie Energétique Nationale – Horizon 2030. ⟨ < http://www.assisesenergie.com/ > ⟩, 2015 (10.12.15).
[16] National Agency for the Development of Renewable Energy and Energy Efficiency (ADEREE). ⟨ < http://www.aderee.ma/ > ⟩.
[17] H.M. Henning, Solar assisted air conditioning of buildings–an overview, Applied thermal engineering 27 (10) (2007) 1734–1749.
[18] TRANSOL. ⟨http://aiguasol.coop/en/transol-solar-thermal-energy software/⟩,. Accessed: December 2015).
[19] IEA SH & C, Task 25 Solar Assisted Air Conditioning of Buildings, Endbericht, 2015
[20] H.M. Henning, Solar assisted air conditioning of buildings–an overview, Applied thermal engineering 27 (10) (2007) 1734–1749.
[21] U. Eicker, Solar Technologies for Buildings, Wilet/Stutgart University of Applied Science, Germany, 2001.
[22] M.D.C. Rodríguez-Hidalgo, P.A. Rodríguez-Aumente, A. Lecuona, M. Legrand, R. Ventas, Domestic hot water consumption vs. solar thermal energy storage: The

optimum size of the storage tank, Applied Energy 97 (2012) 897–906.
[23] A. Allouhi, T. Kousksou, A. Jamil, P. Bruel, Y. Mourad, Y. Zeraouli, Solar driven cooling systems: An updated review, Renewable and Sustainable Energy Reviews 44 (2015) 159–181.
[24] B. Prasartkaew, Performance Test of a Small Size LiBr-H_2O Absorption Chiller, Energy Procedia 56 (2014) 487–497.
[25] A. Shariah, M.A. Al-Akhras, I.A. Al-Omari, Optimizing the tilt angle of solar collectors, Renewable Energy 26 (4) (2002) 587–598.
[26] H.K. Elminir, A.E. Ghitas, F. El-Hussainy, R. Hamid, M.M. Beheary, K.M. Abdel-Moneim, Optimum solar flat-plate collector slope: case study for Helwan, Egypt, Energy Conversion and Management 47 (5) (2006) 624–637.
[27] F. Assilzadeh, S.A. Kalogirou, Y. Ali, K. Sopian, Simulation and optimization of a LiBr solar absorption cooling system with evacuated tube collectors, Renewable Energy 30 (8) (2005) 1143–1159.
[28] S. Bahria, M. Amirat, A. Hamidat, M. El Ganaoui, M. Slimani, Parametric study of solar heating and cooling systems in different climates of Algeria–a comparison between conventional and high-energy-performance buildings, Energy 113 (2016) 521–535.